Arabian Journal of Chemistry (2023) **16**, 104771

King Saud University

Arabian Journal of Chemistry

www.ksu.edu.sa
www.sciencedirect.com

ORIGINAL ARTICLE

Ion exchange pattern-based 18β-glycyrrhetinic acid containing pyridinium salts derivatives as novel antibacterial agents with low toxicity

Jing-Jing He, Ting Li, Hong-Wu Liu, Lin-Li Yang, Yi-Hong Yang, Qing-Qing Tao, Xiang Zhou *, Pei-Yi Wang, Song Yang *

National Key Laboratory of Green Pesticide, Key Laboratory of Green Pesticide and Agricultural Bioengineering, Ministry of Education, Center for R&D of Fine Chemicals of Guizhou University, Guiyang 550025, China

Received 10 January 2023; accepted 27 February 2023
Available online 04 March 2023

KEYWORDS

Pyridinium salts;
Phytotoxicity;
Ion exchange strategy;
Antibacterial activity

Abstract Studies in the past few years have shown that simple salts, such as pyridinium salts and imidazole salts, have excellent antibacterial activity. However, their application in drugs and agrichemicals development has been limited due to their high toxicity. In this study, we found that synthesized target compounds with pyridinium salt unit $\mathbf{A_1}$ and $\mathbf{B_6}$ displayed excellent anti-*Xac* (*Xanthomonas. axonopodis* pv. *citri*) and *Xoo* (*Xanthomonas oryzae* pv. *oryzae*) activity, with EC_{50} values of 7.67 μg/mL and 1.37 μg/mL, respectively. On searching for a toxicity reduction strategy, an ion exchange method was adopted to obtain a new type of various organic acid-decorated pyridinium salt derivatives containing with glycyrrhetinic acid framework, and their structure was characterized by FTIR and ^{1}H NMR. Furthermore, bioassays and toxicity tests were used to show that these organic acid-exchanged compounds not only exhibited lower toxicity to plants but also had excellent antibacterial activity towards virulent phytopathogenic bacteria, especially compound $\mathbf{D_3}$, which provided an EC_{50} of 1.60 μg/mL toward *Xoo*. Subsequently, the pot experiments determined that compound $\mathbf{D_3}$ exhibited suitable protective and curative activities for the management of rice bacterial leaf blight at 200 μg/mL, with control efficacies of 54.09% and 38.50%, respectively. In addition, studies evaluating potential antibacterial mechanisms suggested that apoptosis was responsible for the antibacterial behavior of the target compounds. Overall, this study proved that

Abbreviations: *Xoo*, *Xanthomonasoryzae* pv. *oryzae*; *Xac*, *Xanthomonas axonopodis* pv. *citri*; BT, Bismerthiazol; TC, Thiodiazolecopper; GA, 18β-glycyrrhetinicacid; ROS, Reactive oxygen species; OPO, essentialoiloforangepeel

* Corresponding authors.
E-mail addresses: xiangzhou@gzu.edu.cn, zhoux1534@163.com (X. Zhou), syang@gzu.edu.cn (S. Yang).

Peer review under responsibility of King Saud University.

Production and hosting by Elsevier

https://doi.org/10.1016/j.arabjc.2023.104771

the ion exchange method was a feasible strategy to reduce the toxicity of pyridinium salts and was promising for use in the development of novel antimicrobial agents.

1. Introduction

Plant bacterial diseases refer to physiological lesions of cells and tissues of plants that occur subsequent to being infected with phytopathogenic bacteria. A phenomenon which has occurred in important grain and industrial crops, such as cereals, vegetables, and fruit trees, and are the second most severe plant disease only after fungal infection. In rice production, two common bacterial diseases, bacterial blight and bacterial leaf streak, have been frequently responsible for global outbreaks, seriously affecting an area of 330,000 to 660,000 hm^2 each year, and usually resulting in a yield reduction of about 10% in production (Chen et al., 2021; Hu, 2022; Zhao et al., 2022). Similarly, citrus canker is a notorious bacterial disease in the citrus industry, which can severely affect the citrus tree causing the fruit to drop prematurely, with a significant impact on its economic value. However, this disease is highly contagious and has worried homeowners around the world, and some researchers reported that the field incidence rate could reach 15% in Hunan province, China (Luo et al., 2015; Feng, 2021; Zhang et al., 2021). Furthermore, bacterial wilt in the *Solanaceae* plant is also a devastating disease that can cause a loss of yield of 20% to 50%, and affects peppers, tomatoes, tobacco, and potatoes (Huang et al., 2017; He et al., 2021; Xu et al., 2021). After kiwifruit is infected with canker, local canker rots, causing the tree to weaken; the diseased plant rate is as high as 20% (Li et al., 2013). For all these plants, bacterial diseases have the characteristics of explosiveness, epidemic, destructiveness, and difficulty in control. Therefore, there will be severe damage when plants are infected with bacterial diseases, resulting in a severe reduction in production yields and quality. To date, chemical control has always been the most adopted and efficient measure in most cases of epidemics. However, because the long-term continuous use and abuse of a small variety of chemical agents, including cupric pesticide, streptomycin sulfate, and bismerthiazol (BT), not only leads to a series of environmental and ecological problems, such as increased resistance of phytopathogenic bacteria, excessive pesticide residues, and soil and water pollution, but also seriously affects the safety of agricultural products (Wang et al. 2022). Under the background of "China's 14th Five-Year Plan," green agricultural development has become the dominant direction of future agriculture. Thus, the development of efficient, green, and environmentally friendly agrochemicals has become a great challenge (Chen and Chen, 2022).

The chemical modification of active natural products has strongly motivated the discovery and development of new pesticides and medicines (Butler, 2005; Camp et al., 2012; Hüter, 2011; Joo, 2014; Marrone, 2019; Wu et al., 2019). 18β-glycyrrhetinic acid (GA), a pentacyclic triterpenoid, is an active ingredient extracted from the rhizomes of *Glycyrrhiza uralensis Fisch* and other plants (Song et al., 2022), which has attracted a great deal of attention due to its extensive applications in food additives, cosmetics, matrix materials and medicine (Jager et al., 2009; Xu et al., 2012; Zhang et al., 2013; Huang et al., 2018). In addition, GA is an ideal lead compound; it not only exhibits diverse bioactive activities including anti-inflammatory (Radwan et al., 2016), antiviral (Zígolo et al., 2018), antibacterial (Yang et al., 2020), and antitumor (Sun et al., 2019) activities, but also has a modifiable chemical structure, given a hydroxyl group at the 3-position, an unsaturated ketone at the 11- and 13-positions, and a carboxyl group at the 20-position (Gaware et al., 2011; Hussain et al., 2018). However, some undesirable physical and chemical properties of GA have severely limited its application prospects, such as high hydrophobicity, low bioavailability, poor water solubility, and permeability (Tian et al. 2012; Lei et al. 2016; Dai et al., 2018). As for the derivatives of pyridinium salts, a quaternary ammonium salt has been suggested, which exhibits excellent antibacterial (Zhao and Sun, 2006; Sundararaman et al., 2013), anticancer (Fahs et al., 2014), and other biological activities, and can also be used as a surfactant (Zhen et al., 2011) (Fig. 1). Many studies have verified that salt-based antibacterial agents based on pyridinium have excellent water solubility and are relatively less toxic to mammalian cells, but are highly toxic to microorganisms and some plants, and may be the main reason for their rarely reported antibacterial agent in agricultural production (Chen et al., 2019). More interestingly, through the use of rational molecule modification, some pyridinium salt derivatives not only have outstanding antibacterial competence but have also exhibit low toxicity to nontarget organisms. Therefore, further investigation is needed to identify new functions and applications of pyridinium salt derivatives.

Hence, to improve the water solubility and bioactivity of GA, a series of pyridinium salt-based GA derivatives were prepared, and their *in vitro* and *in vivo* antibacterial activities and primary antibacterial mechanisms were studied using a series of biochemical assays. Furthermore, an ion exchange method was employed to successfully reduce their phytotoxicity.

2. Materials and methods

2.1. Instruments and chemicals

The NMR spectra of the title compounds were obtained on a JEOL-ECX500 apparatus (Akishima, Japan) or a Bruker Biospin AG-400 apparatus (Bruker Optics, Germany) using TMS as the internal standard. HRMS spectra were obtained on a Q-Exactive Orbitrap MS apparatus (Thermo Fisher Scientific, USA). Infrared (IR) spectra were collected using a Fourier transform infrared spectrometer (Thermo Scientific Nicolet iS50, Thermo Fisher Scientific). A Nova Nano SEM 450 instrument captured scanning electron microscope (SEM) images. Fluorescent images were collected using an Olympus BX53 microscope (Olympus, Tokyo, Japan). Optical density was recorded on a Cytation™ 5 multi-mode readers (BioTek Instruments, Inc. USA). 18β-Glycyrrhetinic acid (purity > 97%) was purchased from Energy Chemical of Saen Chemical Technology (Shanghai) Co., Ltd.

2.2. Experimental section

For *in vitro* antibacterial bioassays, apoptosis responses, ROS detection, fluorescent images, and enzyme activity assays were performed as described in our previous studies (Zhao et al., 2019, Wang et al., 2020; Xiang et al., 2020).

2.3. Toxicity assays of compound D_3 in rice plant

The toxicity assay of compound $\mathbf{D_3}$ was conducted based on our reported method with slight modifications. Briefly, rice plants (Fengyouxiangzhan variety) grown at the maximum leaf stage were used in this experiment. Then, compounds $\mathbf{B_6}$ and $\mathbf{D_3}$ were prepared in sterile water at the final concentration

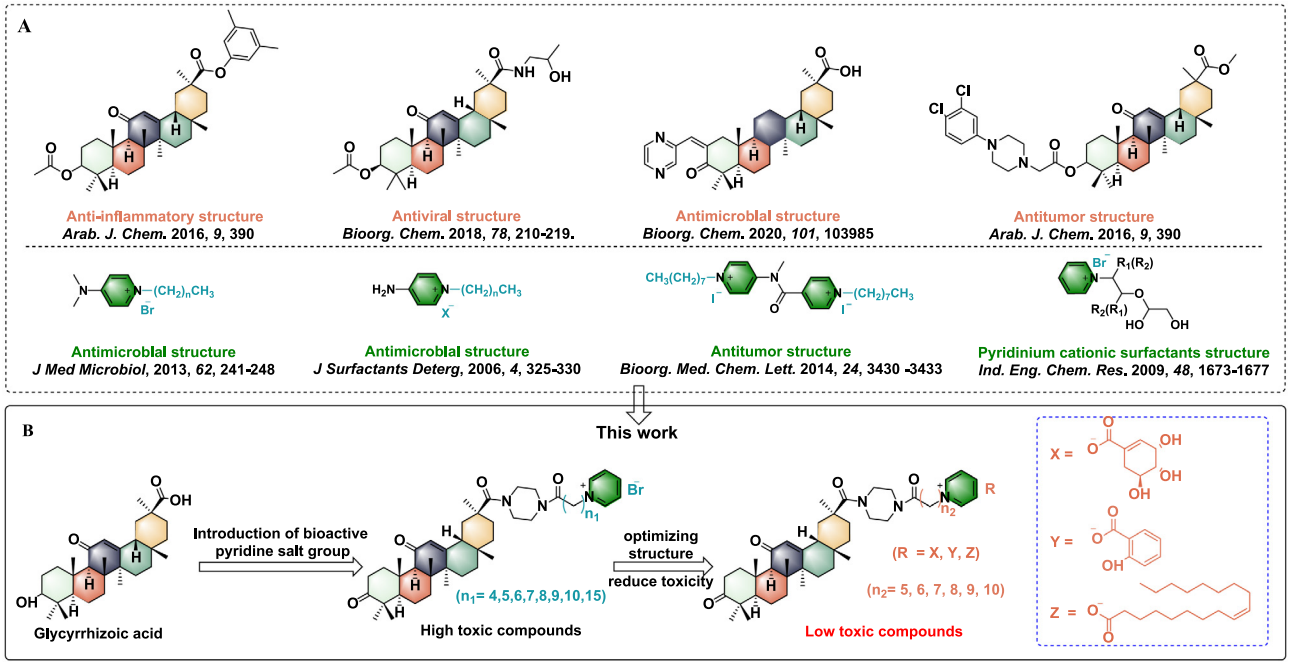

Fig. 1 **A**) Reported bioactive molecules containing 18β-glycyrrhetinic acid or pyridine salt; **B**) The design strategy for target molecules.

of 200 μg/mL. Subsequently, 20 mL volumes of the solutions were evenly sprayed on rice leaves and grown in a greenhouse. Finally, the condition of the rice leaves was observed 14 days after spraying. Each experiment was performed in duplicate, and rice plants treated only with an equivalent amount of sterile water and grown under the same conditions were used as a blank control.

2.4. In vivo bioassay against rice bacterial blight

The *in vivo* antibacterial activities of compound **D_3** against rice bacterial leaf blight were performed based on our reported method with some modifications (Huang et al., 2021). Bismerthiazol (BT, 90% technical material) and thiodiazole copper (TC, 20% suspending agent) were used as positive controls, and rice plants (variety Fengyouxiangzhan) cultured in a greenhouse for 2 months were used. For protective assays, different adjuvants were added to a compound **D_3** solution at 200 μg/mL to obtain a mixture that included essential oil of orange peel (OPO) at a dose of 0.1% (v/v). Then 20 mL of the solution was evenly sprayed onto the rice leaves and the *Xoo* cell solution (OD_{595} = 0.6–0.8) was inoculated using the leaf clipping method at 24 h after spraying. To determine the curative activity, *Xoo* cells were first inoculated and then the mixture was sprayed 24 h after inoculation. All treatments were cultured in a climate chamber (95% RH) with 16 h lighting at 28 °C and 8 h dark at 25 °C. The results were observed 14 days after inoculation.

2.5. Dual AO/EB fluorescent staining

Acridine orange/ethidium bromide (AO/EB) staining was conducted using Kasibhatla et al.'s method with some modifications (Kasibhatla et al., 2006). Briefly, 2 mL of *Xoo* culture solution (OD_{595} = 0.6–0.8) was exposed to compound **D_3** at different concentrations at 28 °C for 12 h. Subsequently, the treated *Xoo* cells were collected by centrifugation (6000 × g, 5 min, 4 °C), washed with sterile water (1 mL × 2), then resuspended in sterile water (1 mL) and the supernatant was discarded. For compound **D_3** treatments or control were then mixed with 5 μL of the dye mixture of AO (10 μg/mL)/EB (100 μg/mL) in the ratio of 1: 1 and incubated at 28 °C for 20 min with *Xoo* cells. Subsequently, 1 mL of sterile water, was added, mixed well, resuspended, and the supernatant was discarded. Finally, all samples were observed and immediately captured using an Olympus BX53 microscope (Olympus, Tokyo, Japan).

*2.6. Accumulation of reactive oxygen species triggered by target compound **D_3***

The reactive oxygen species (ROS) content in **D_3**-triggered pathogens (*Xoo*) was measured using an ROS assay kit (Beyotime Institute of Biotechnology, Haimen, China). Briefly, 1 mL of *Xoo* culture solution (OD_{595} = 0.6–0.8) was exposed to compound **D_3** at different concentrations at 28 °C for 12 h. Subsequently, *Xoo* cells (OD_{595} is 0.6–0.8) were collected by centrifugation (6000 × g, 5 min, 4 °C), washed with sterile water (1 mL × 2), and resuspended in sterile water (1 mL). Finally, 0.5 mL of the resuspended solution was mixed with 1 μL of the Beyotime dyeing solution in a dark environment for 20 min, and all samples were observed and captured with an Olympus BX53 microscope (Olympus, Tokyo, Japan).

3. Results and discussion

*3.1. Synthesis and antibacterial activity of target compounds **A_1-A_7** and **B_1-B_7***

The synthetic route and structure of pyridinium salt-decorated 18β-glycyrrhetinic derivatives possessing flexible alkyls are illustrated in Scheme 1. Briefly, the piperazine group was first

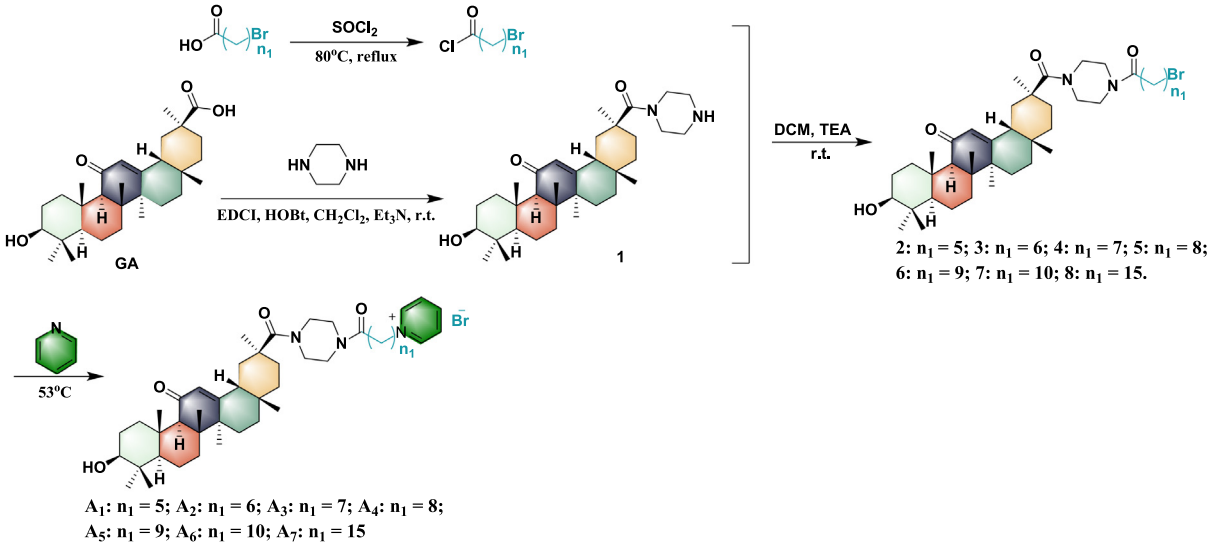

Scheme 1 Synthesis of pyridine salt-decorated 18β-glycyrrhetinic acid derivatives $\mathbf{A_1}$-$\mathbf{A_7}$.

introduced into the 30-position of carbon of GA via a classical condensation reaction to provide intermediate **1**. Then, key intermediates **2**–**8** were prepared by a substitution reaction between acyl chloride containing different alkyl chain lengths and intermediate **1**. Finally, target molecules ($\mathbf{A_1}$-$\mathbf{A_7}$) were obtained by a substitution reaction between intermediates **2**–**8** and pyridine at 53 °C. In addition, target compounds $\mathbf{B_1}$-$\mathbf{B_7}$ were synthesized using a route similar to (Scheme 2) to compounds $\mathbf{A_1}$-$\mathbf{A_7}$. In summary, intermediates **2**–**8** were oxidized to obtain intermediates **9**–**15**, which were then substituted with pyridine at 53 °C to obtain the target compounds $\mathbf{B_1}$-$\mathbf{B_7}$. All molecular structures were confirmed by ^{1}H NMR, ^{13}C NMR, and HRMS (for detailed information see the supplementary data Figs. S1-S87). Bioassays of the target compounds against phytopathogenic bacteria were evaluated using the turbidimeter test. The results of the bioassay indicated that some of the synthesized compounds displayed remarkable antibacterial activity against phytopathogenic bacteria, including *Xanthomonas oryzae* pv. *oryzae* (*Xoo*) and *X. axonopodis* pv. *citri* (*Xac*) (Table 1). In detail, most target molecules ($\mathbf{A_1}$-$\mathbf{A_7}$ and $\mathbf{B_1}$-$\mathbf{B_7}$) showed vastly improved antibacterial activity of GA (EC_{50} > 100 μg/mL) against anti-*Xoo* and anti-*Xac*, with EC_{50} values ranging from 1.37 to 64.80 μg/mL, which suggested that the pyridinium salts moiety was a key pledge to improve antibacterial potency. The best antibacterial activity against *Xac* was compound $\mathbf{A_1}$ whose 3-hydroxyl group was not oxidized, with an EC_{50} value of 7.67 μg/mL. Next, the 3-position hydroxyl group of 18β-glycyrrhetinic acid was oxidized to a series of target compounds, with the growth of the flexible alkyl chain, the anti-*Xoo* EC_{50} value showed a trend of first increasing and then decreasing. Of these, compounds with chain lengths of 8, 9,

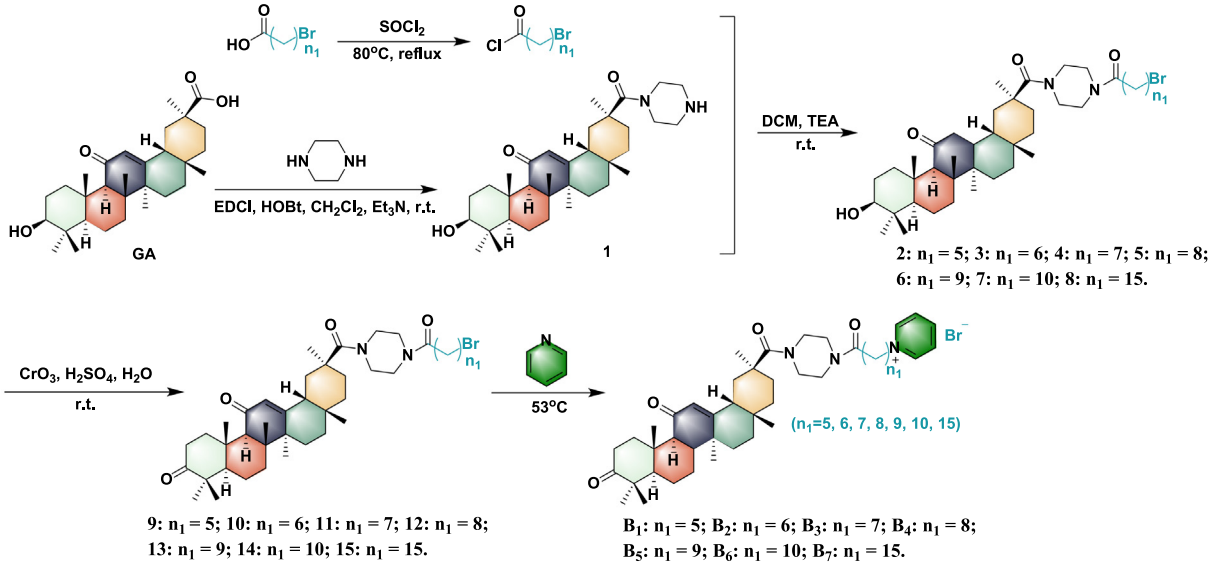

Scheme 2 Synthesis of pyridine salt-decorated 18β-glycyrrhetinic acid derivatives $\mathbf{B_1}$-$\mathbf{B_7}$.

Table 1 *In vitro* bioassay results of **1–15, A_1-A_7, and B_1-B_7** against plant pathogens *Xoo* and *Xac*.

Compd.	*Xoo*		*Xac*	
	regression eq.	EC_{50}(μg/mL)	regression eq.	EC_{50}(μg/mL)
GA	–	> 100	–	> 100
1	y = 5.403x − 0.099	8.78 ± 0.69	y = 0.927x + 3.865	16.70 ± 1.27
2	–	> 100	y = 1.263x + 3.203	26.40 ± 1.73
3	–	> 100	–	> 100
4	–	> 100	y = 0.440x + 4.230	56.00 ± 5.85
5	–	> 100	y = 1.271x + 3.341	20.20 ± 0.83
6	–	> 100	–	> 100
7	–	> 100	–	> 100
8	–	> 100	–	> 100
9	–	> 100	–	> 100
10	–	> 100	–	> 100
11	–	> 100	–	> 100
12	–	> 100	–	> 100
13	–	> 100	–	> 100
14	–	> 100	–	> 100
15	–	> 100	–	> 100
A_1	y = 5.835x + 0.443	8.57 ± 1.05	y = 1.784x + 3.421	7.67 ± 0.32
A_2	y = 2.214x + 3.406	5.24 ± 0.76	y = 1.659x + 3.374	9.55 ± 0.52
A_3	y = 2.690x + 3.106	5.06 ± 0.47	y = 0.490x + 4.553	8.16 ± 0.74
A_4	y = 2.898x + 3.410	3.54 ± 0.20	y = 1.459x + 3.521	10.30 ± 0.12
A_5	y = 4.965x + 2.317	3.47 ± 0.28	y = 0.387x + 4.406	34.10 ± 3.41
A_6	y = 12.62x − 5.340	6.60 ± 0.67	y = 1.002x + 3.756	17.40 ± 1.05
A_7	–	> 100	–	> 100
B_1	y = 3.743x + 1.345	9.47 ± 0.94	y = 0.945x + 3.986	11.80 ± 0.28
B_2	y = 6.376x − 1.139	9.18 ± 0.98	y = 1.044x + 3.394	34.50 ± 2.17
B_3	y = 8.796x − 2.497	7.12 ± 0.15	y = 2.354x + 2.694	9.53 ± 1.18
B_4	y = 4.618x + 2.557	3.38 ± 0.10	y = 0.686x + 4.127	18.70 ± 2.31
B_5	y = 8.480x + 1.950	2.29 ± 0.29	y = 0.614x + 4.134	25.60 ± 2.52
B_6	y = 5.794x + 4.211	1.37 ± 0.03	y = 0.391x + 4.385	37.40 ± 2.60
B_7	–	> 100	–	> 100
BT	y = 1.289x + 2.898	42.60 ± 3.11	–	> 100
TC	y = 2.819x − 0.856	119.44 ± 2.54	y = 7.726x − 9.949	86.09 ± 2.87

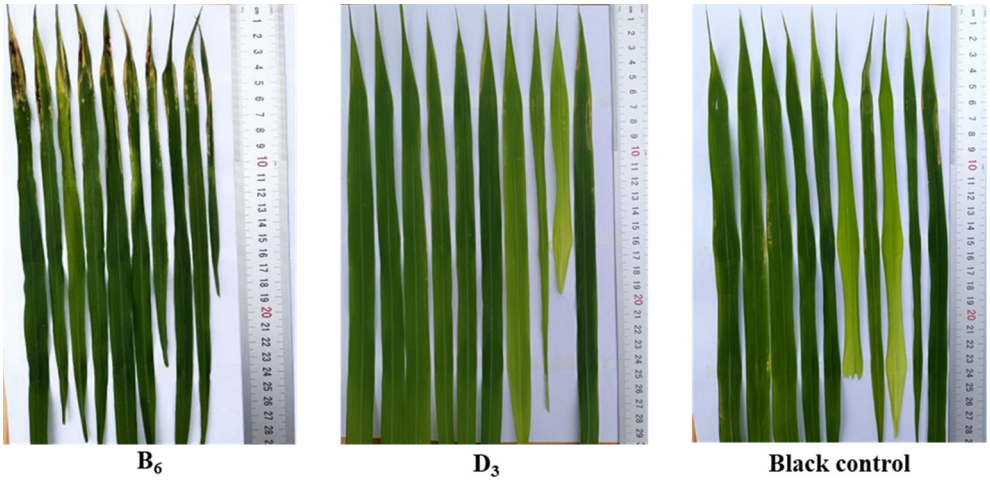

Fig. 2 *In vivo* phytotoxicity test of **B_6**, **D_3**, and CK in rice under greenhouse conditions at 200 μg/mL.

and 10 (corresponding to compounds **B_4**, **B_5**, and **B_6**) exhibited EC_{50} values of 3.38, 2.29 and 1.37 μg/mL, respectively. Furthermore, compounds with flexible alkyl chain lengths of 5, 6, and 7 (corresponding to compounds **A_1**, **A_2**, and **A_3**) showed more significant inhibition of *Xac* growth, affording EC_{50} values of 7.67, 9.55 and 8.16 μg/mL, respectively. Further studies

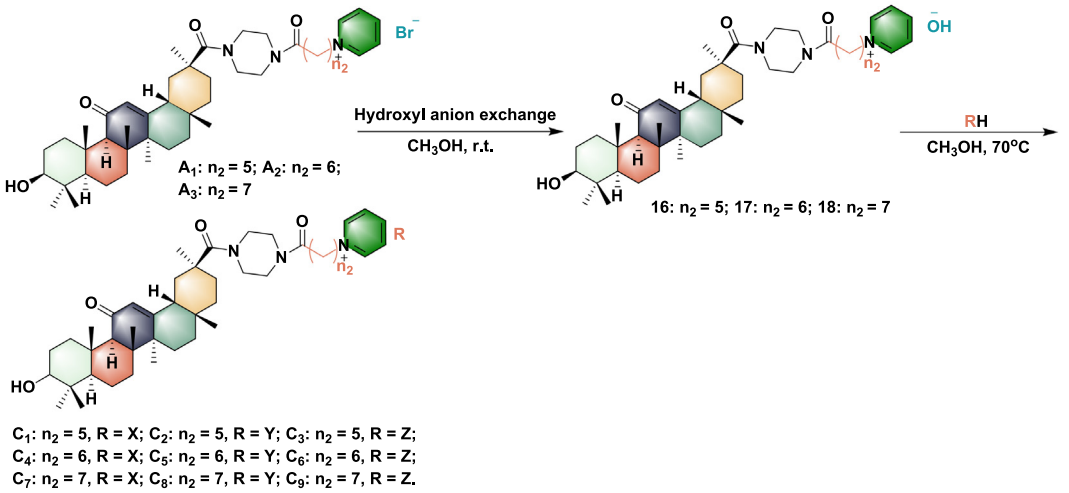

Scheme 3 Synthesis of optimized compounds C_1-C_9.

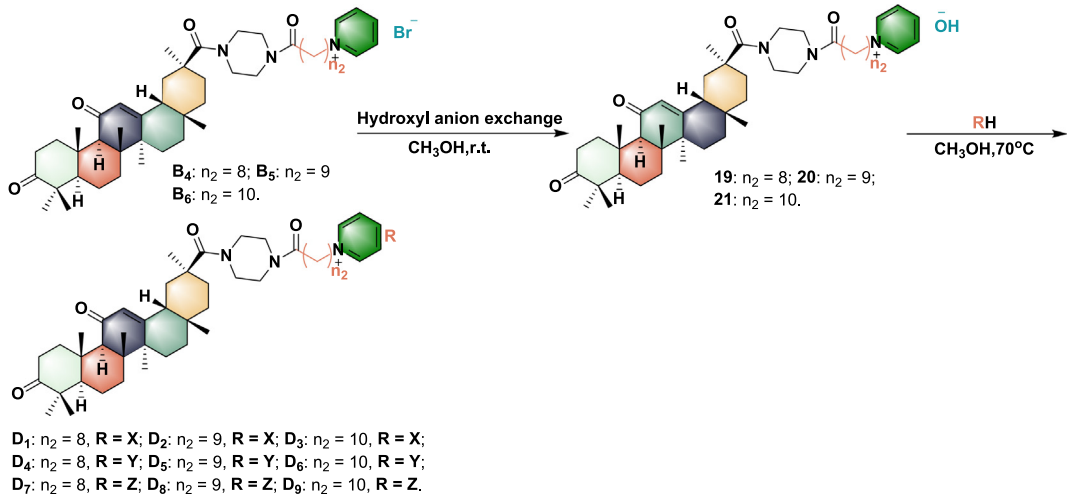

Scheme 4 Synthesis of optimized compound D_1-D_9.

Table 2 *In vitro* bioassay results of C_1-C_9 against plant pathogens *Xoo* and *Xac*.

Compd.	*Xoo*		*Xac*	
	regression eq.	EC_{50} (μg/mL)	regression eq.	EC_{50} (μg/mL)
C_1	y = 2.208x + 2.463	14.08 ± 1.50	y = 2.327x + 2.279	14.76 ± 0.53
C_2	y = 3.254x + 0.799	19.53 ± 1.66	y = 1.676x + 3.604	6.80 ± 0.45
C_3	y = 1.189x + 3.477	19.06 ± 2.17	y = 0.961x + 4.363	4.59 ± 0.70
C_4	y = 1.014x + 3.901	12.11 ± 2.41	y = 1.964x + 3.354	6.88 ± 0.60
C_5	y = 2.312x + 2.431	12.90 ± 0.70	y = 5.272x − 2.372	25.03 ± 1.66
C_6	y = 1.816x + 2.614	20.59 ± 2.14	y = 1.143x + 3.792	11.40 ± 1.74
C_7	y = 1.983x + 3.383	6.5 ± 1.16	y = 1.400x + 3.360	14.81 ± 0.75
C_8	y = 1.400x + 3.360	6.17 ± 2.30	y = 1.735x + 3.147	11.69 ± 0.73
C_9	y = 1.676x + 3.604	17.25 ± 0.03	y = 1.767x + 2.953	14.39 ± 0.83
BT	y = 1.289x + 2.898	42.60 ± 3.11	–	> 100
TC	y = 2.819x − 0.856	119.44 ± 2.54	y = 7.726x − 9.949	86.09 ± 2.87

Table 3 *In vitro* bioassay results of $\mathbf{D_1}$-$\mathbf{D_9}$ against plant pathogens *Xoo* and *Xac*.

Compd.	*Xoo*		*Xac*	
	regression eq.	EC_{50} (μg/mL)	regression eq.	EC_{50} (μg/mL)
$\mathbf{D_1}$	y = 1.388x + 4.009	5.17 ± 0.54	y = 2.074x + 3.226	7.16 ± 0.67
$\mathbf{D_2}$	y = 2.075x + 4.156	4.18 ± 0.09	y = 3.194x + 1.774	10.23 ± 0.79
$\mathbf{D_3}$	y = 2.094x + 4.575	1.60 ± 0.34	y = 0.325x + 4.698	8.48 ± 0.07
$\mathbf{D_4}$	y = 1.717x + 3.810	4.93 ± 0.93	y = 1.703x + 1.936	3.82 ± 0.14
$\mathbf{D_5}$	y = 1.009x + 4.113	7.56 ± 0.75	y = 1.909x + 3.775	4.38 ± 0.61
$\mathbf{D_6}$	y = 8.912x − 0.498	4.14 ± 0.20	y = 2.253x + 2.733	10.15 ± 0.20
$\mathbf{D_7}$	y = 2.373x + 2.296	13.77 ± 0.63	y = 2.063x + 2.224	22.17 ± 1.29
$\mathbf{D_8}$	y = 1.781x + 3.048	12.46 ± 0.08	y = 1.658x + 4.475	2.07 ± 0.58
$\mathbf{D_9}$	y = 1.899x + 4.099	2.98 ± 0.39	y = 0.763x + 4.516	6.08 ± 0.19
BT	y = 1.289x + 2.898	42.60 ± 3.11	–	>100
TC	y = 2.819x − 0.856	119.44 ± 2.54	y = 7.726x − 9.949	86.09 ± 2.87

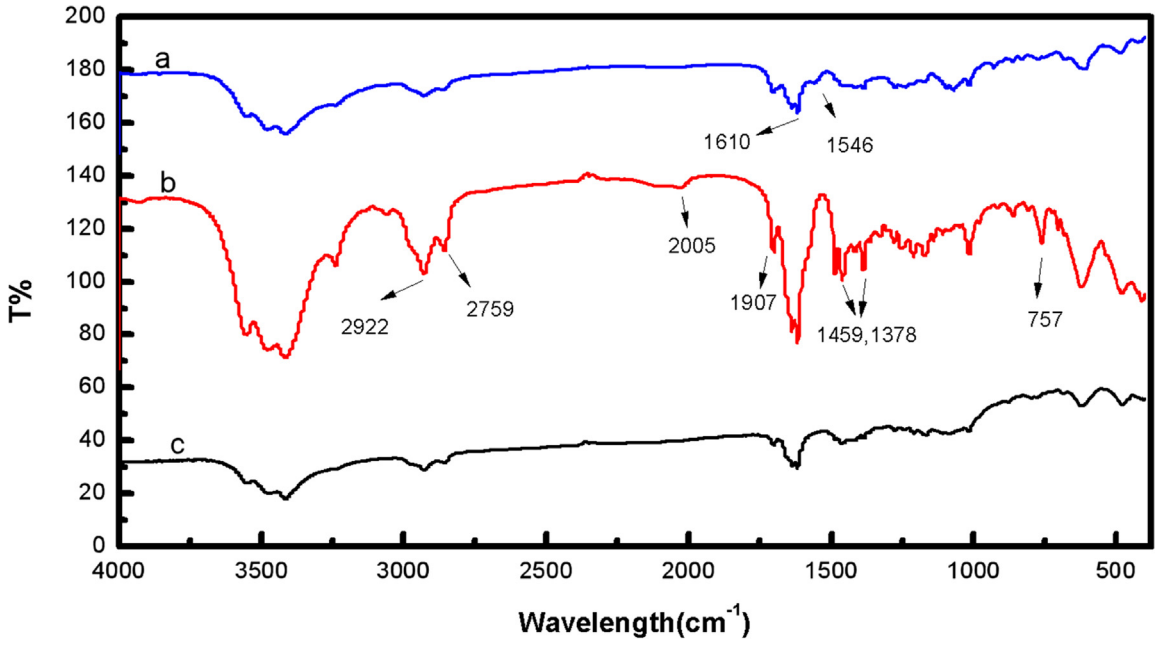

Fig. 3 FTIR spectra of compounds (a) $\mathbf{D_4}$, (b) $\mathbf{D_3}$, and (c) $\mathbf{B_6}$.

showed that this ability was increased against *Xoo* and decreased against *Xac*, while the 3-position hydroxyl group of compounds $\mathbf{A_1}$-$\mathbf{A_7}$ was oxidized to the carbonyl group (compounds $\mathbf{B_1}$-$\mathbf{B_7}$). Based on the bioassay results, we found that the pyridine salt moiety played an extremely important role in enhancing antibacterial activity.

3.2. Synthesis, antibacterial activity, and rice leaf toxicity test of further optimized compounds $\boldsymbol{C_1}$-$\boldsymbol{C_9}$ *and* $\boldsymbol{D_1}$-$\boldsymbol{D_9}$

Based on the bioassay results of the compounds in series A and B, molecule $\mathbf{B_6}$ with the highest activity (EC_{50} = 1.37 μg/mL to anti-*Xoo*) was chosen to perform the phytotoxicity test on the rice plant. The results showed (Fig. 2) that compound $\mathbf{B_6}$ exhibited marked toxicity for the rice plant and produced a large number of black spots on the rice leaves 14 days after spraying at 200 μg/mL. Meanwhile, we found that some quaternary ammonium compounds were very effective against both Gram-positive and Gram-negative bacteria, but they were also quite toxic (Schoenberg et al., 1974; Thorsteinsson et al., 2003). Bodor et al. (1980) proposed that the toxicity of quaternary ammonium surfactants is mainly related to various biological effects of the quaternary ammonium head and its metabolites (such as oxidative dealkylation). Thus, they designed and synthesized a new class of "soft antibacterial agents" containing ester moieties to prevent and reduce drug-related toxicity effects, which cleaved into non-toxic moieties by chemical or enzyme hydrolysis after exerting antibacterial effects. Encouraged by these findings, to reduce phytotoxicity, an ion exchange method was adopted to optimize the structure of six active compounds $\mathbf{A_1}$, $\mathbf{A_2}$, $\mathbf{A_3}$, $\mathbf{B_4}$, $\mathbf{B_5}$, and $\mathbf{B_6}$. In detail, the ion exchange first involved switching between the bromide anion and hydroxide anion in the methanol solution at room temperature to obtain the key intermediates **16**–**21**. Then, salicylic acid, shikimic acid, and oleic acid were sequentially introduced in anhydrous methanol at 70

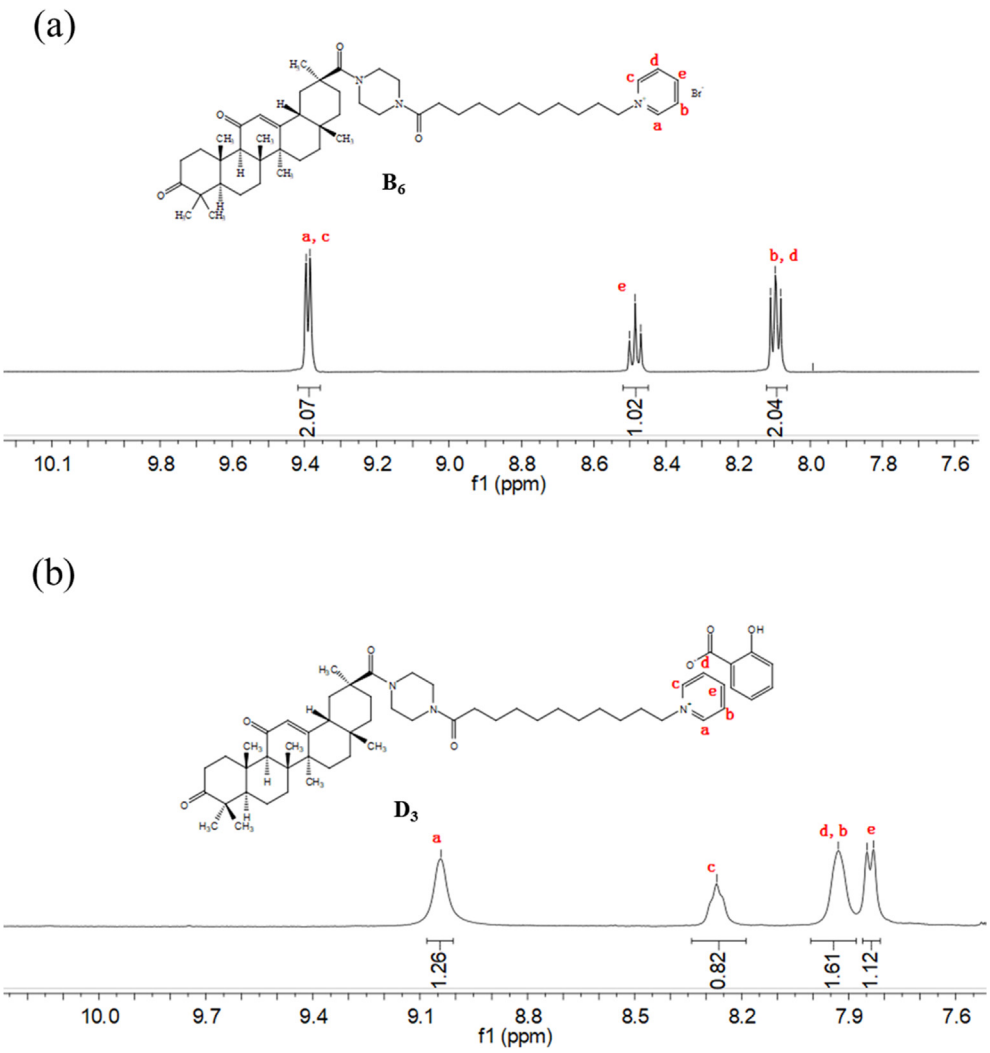

Fig. 4 ^{1}H NMR confirmed the structures of compounds (a) **B_6** and (b) **D_3**.

°C, and a class of novel pyridinium salt-decorated 18β-glycyrrhetinic derivatives (**C_1-C_9 and D_1-D_9**) were formed via two-step reactions (Schemes 3 and 4). Furthermore, *in vitro* bioassays (shown in Tables 2 and 3) indicated that compounds with different acids, i.e., compounds **A_1**, **A_2**, **A_3**, **B_4**, **B_5**, and **B_6**, could effectively enhance anti-*Xac* ability. In particular, compound **D_8** provided an EC_{50} = 2.07 μg/mL toward anti-*Xac*, which was significantly higher than that of the corresponding compound **A_1** (EC_{50} = 7.67 μg/mL). Meanwhile, as for anti-*Xoo*, the antibacterial activities of optimized compounds were basically maintained. Of these, compounds **D_3** and **D_9** achieved more significant effects, with EC_{50} values of 1.60 and 2.98 μg/mL, respectively. In addition, compounds with alkyl chain lengths of 10 were more dominant in anti-*Xoo* than other alkyl chain lengths. Furthermore, the phytotoxicity test of active compound **D_3** (EC_{50} = 1.60 μg/mL to anti-*Xoo*) was evaluated in rice plants. The results indicated (Fig. 2) that compound **D_3** did not produce any adverse impact on rice leaves 14 days after spraying at 200 μg/mL. Altogether the results suggested that the ion exchange method was a feasible strategy to reduce the phytotoxicity of pyridinium salts while effectively maintaining the antibacterial potency.

*3.3. Structural characterization of compounds **B_6**, **D_3**, and **D_4***

FTIR was used to monitor the functional groups of compounds **B_6** and **D_3**. The FTIR spectra (Fig. 3) of compounds **D_3** and **B_6** presented peaks at 2922 and 2759 cm^{-1} which were attributed to the H-stretch vibration of the pyridine ring, and peaks at 1709 and 1610 cm^{-1} indicated the characteristic absorption of the carbonyl group at the 3-position and α, β-unsaturated ketones at the 11,12 position of the 18β-glycyrrhetinic acid skeleton. As shown in Fig. 3**b**, the spectrum of **D_3** showed the in-plane bending vibration absorption of the benzene ring C–H and the *ortho*-disubstituted characteristic absorption of the benzene ring skeleton, with peaks at 1459, 1378, and 757 cm^{-1}. Furthermore, a weak absorption band appeared at 2005 cm^{-1} that was assigned to the overtone peak of the benzene ring of compound **D_3**. Regarding compound **D_4**, an absorption peak (Fig. 3**a**) appeared at 1546 cm^{-1}, which was attributed to the characteristic absorption of the shikimic acid double bond. Altogether these FTIR data indicated that salicylic acid and shikimic acid were successfully introduced into compounds **D_3** and **D_4**, respectively. Furthermore, the structure of these

newly synthesized compounds (compound **B_6** and **D_3**) was also confirmed by ^{1}H NMR (as shown in Fig. 4). The chemical shifts of the protons around the pyridine nitrogen atoms shifted to a high field after the bromide ion was exchanged for other acid anions, which may be due to the electron cloud density being increased by hydrogen bonding or electrostatic attraction. The spectroscopy evidence indicated that the different acid anions were successfully introduced and that the acid anions were probably arranged around the pyridinium cations by a series of intermolecular interactions.

3.4. In vivo bioassay against rice bacterium blight

To validate the potential application of compound **D_3** in the management of plant bacterial diseases, an *in vivo* bioassay against rice bacterial blight was assessed using a pot experiment under greenhouse conditions. Meanwhile, 0.1% (v/v) orange peel essential oil (OPO) was added to improve the surface wettability of compound **D_3** in rice leaves, which aims to reduce losses during spraying and increase efficacy. As shown in Fig. 5 and Table 4, compound **D_3** could effectively control

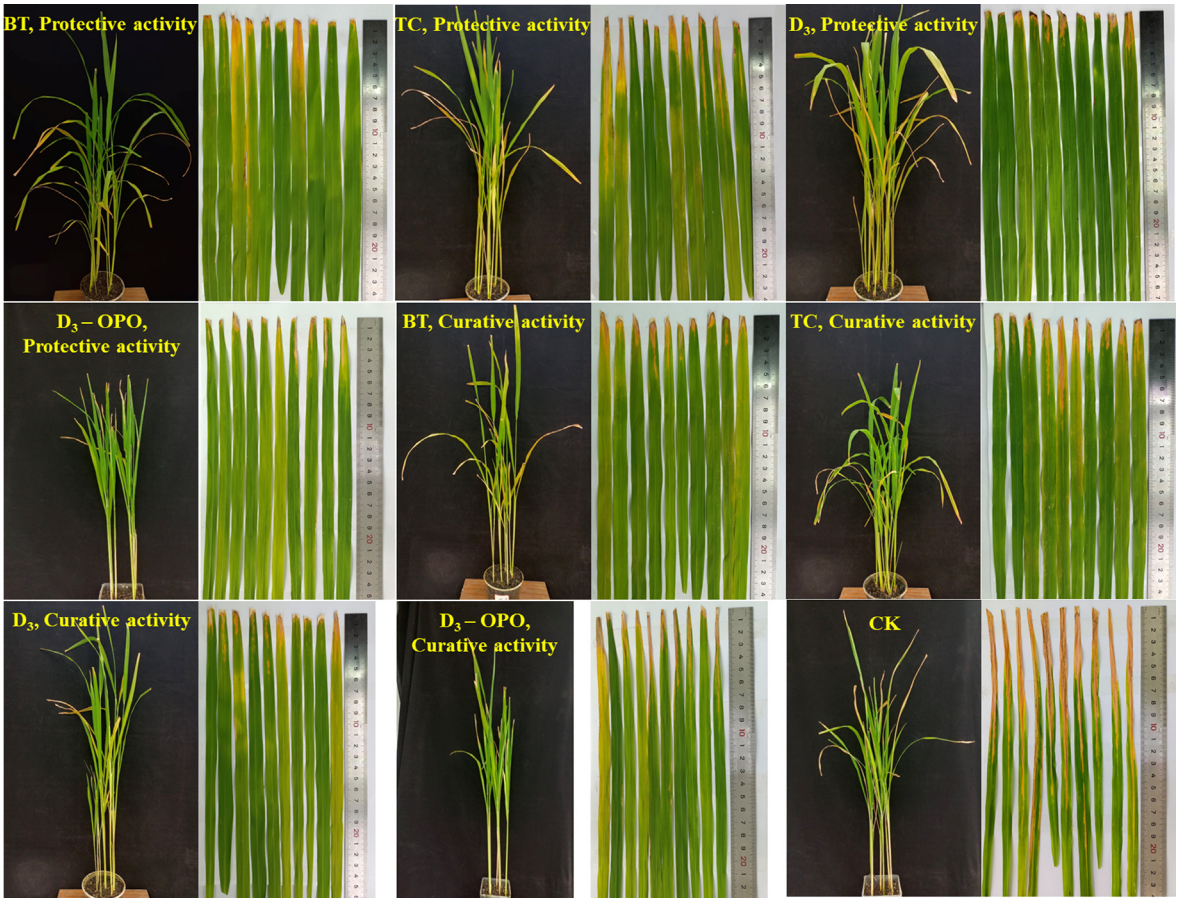

Fig. 5 Curative and protective activities of compounds **D_3**, **BT**, and **TC** against rice bacterial blight under greenhouse conditions at 200 μg/mL.

Table 4 Curative and protective activities (dosage: 200 μg/mL, 14 days after spraying) of **D_3** against rice bacterial blight.

Chemicals	Protect activity			Curative activity		
	Morbidity (%)	Disease index (%)	Control efficiency[b] (%)	Morbidity (%)	Disease index (%)	Control efficiency[b] (%)
D_3	100	40.48	54.09B	100	54.67	38.50B
D_3-OPO	100	40.00	54.62A	100	47.14	46.52A
TC	100	49.52	43.82D	100	57.33	35.50D
BT	100	49.33	44.04C	100	56.00	37.00C
CK[a]	100	88.15		100	88.89	

[a] Negative control.

[b] Statistical analysis was conducted using the ANOVA method under the condition of equal variances assumed ($P > 0.05$) and equal variances not assumed ($P < 0.05$). Different uppercase letters indicate the control efficiencies with significant differences among other treatment groups at $p < 0.05$.

rice bacterial blight at 200 μg/mL with protective and curative activities of 54.09% and 38.50%, respectively, which were much better than commercial bactericides **BT** (44.04% and 37.00%) and **TC** (43.82% and 35.50%). Expectedly, the protective activity (54.62%) and curative activity (46.52%) of compound $\mathbf{D_3}$ were mildly enhanced after adding 0.1% OPO. Altogether, these findings suggested that 18-glycyrrhetinic derivatives coated with pyridinium salt-decorated 18β-glycyrrhetinic derivatives were powerful alternatives for protecting plants from bacterial infections, and the addition of OPO could effectively promote the potency.

3.5. Acridine orange/ethidium bromide (AO/EB) staining to detect apoptosis

Acridine orange (AO)/ethidium bromide (EB) double staining assay was used to observe the apoptosis of *Xoo* cells triggered by compound $\mathbf{D_3}$. AO is a fluorescent nucleic acid cationic dye that can stain live and dead cells, causing cells to emit bright green fluorescence. EB can only penetrate cells with damaged membranes, causing cells to emit orange fluoresce. Apoptotic cells displayed an orange fluorescence in a merged image when dyed using the AO/EB double staining method (Guo, 1998). Thus, a fluorescence microscope was used to observe the experimental results of AO/EB double staining in this study and the results showed that the *Xoo* cell treated with compound $\mathbf{D_3}$ emitted bright red fluorescence after staining with AO/EB, while the control group only emitted green fluorescence, indicating that compound $\mathbf{D_3}$ could cause certain damage to the cytomembrane of *Xoo* cells. Meanwhile, with increased concentration of compound $\mathbf{D_3}$, the intensity of red and orange fluorescence had obviously increased, but a visible decrease was observed in green fluorescence (Fig. 6), which indicated that the degree and amount of damaged and apoptotic cells increased evidently with increasing concentration of compound $\mathbf{D_3}$. These results suggested that our designed compound could induce the cell apoptosis of phytopathogenic bacteria.

3.6. Fluorescence imaging of dichlorofluorescein from ROS-induced Xoo pathogen

Excess ROS is a crucial factor in triggering the apoptosis (Mehraj et al., 2022), so the accumulation of ROS in *Xoo*

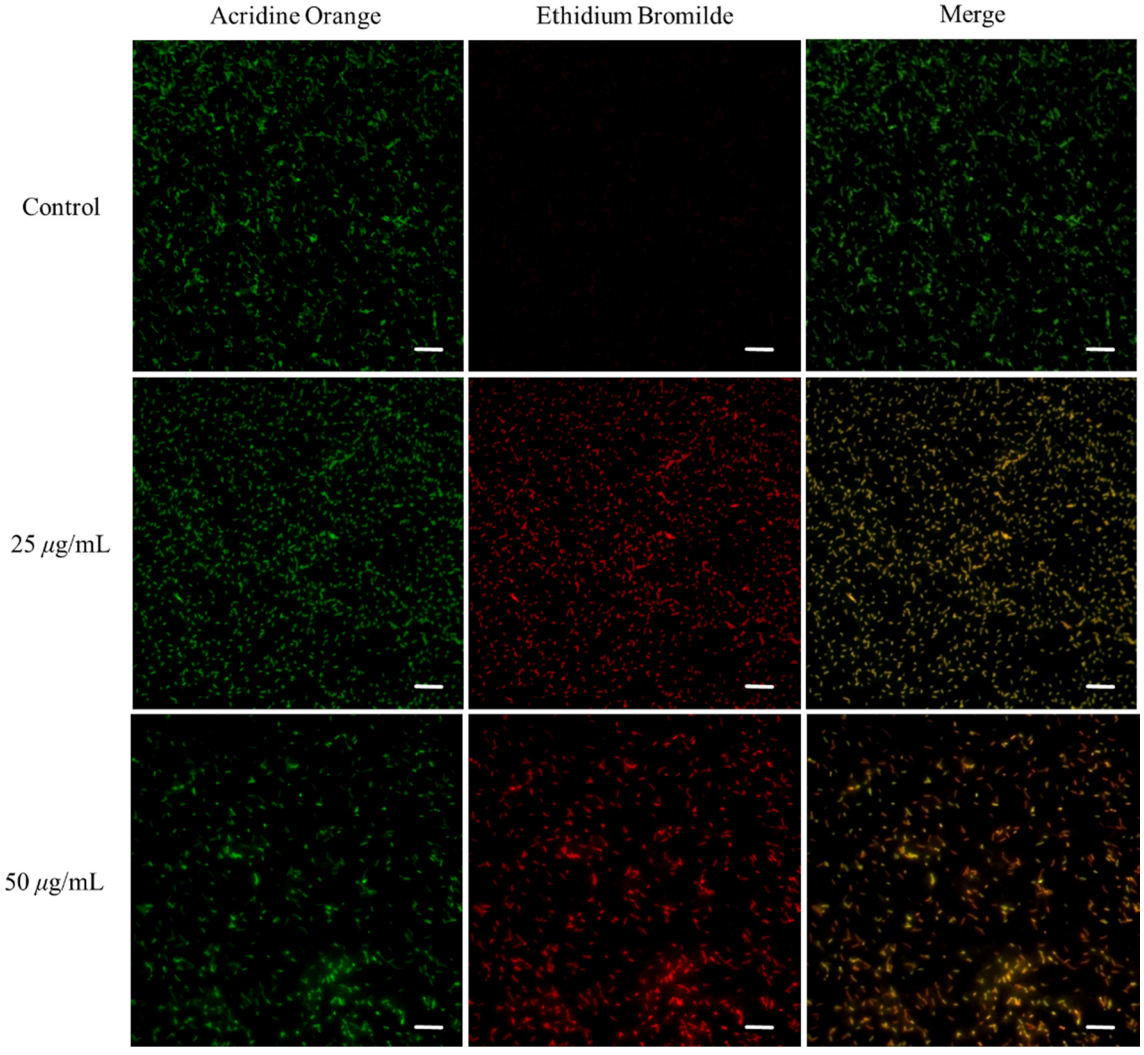

Fig. 6 AO/EB dual fluorescence staining results for *Xoo* after incubation with $\mathbf{D_3}$ for 12 h. All the scale bars for are 10 μm.

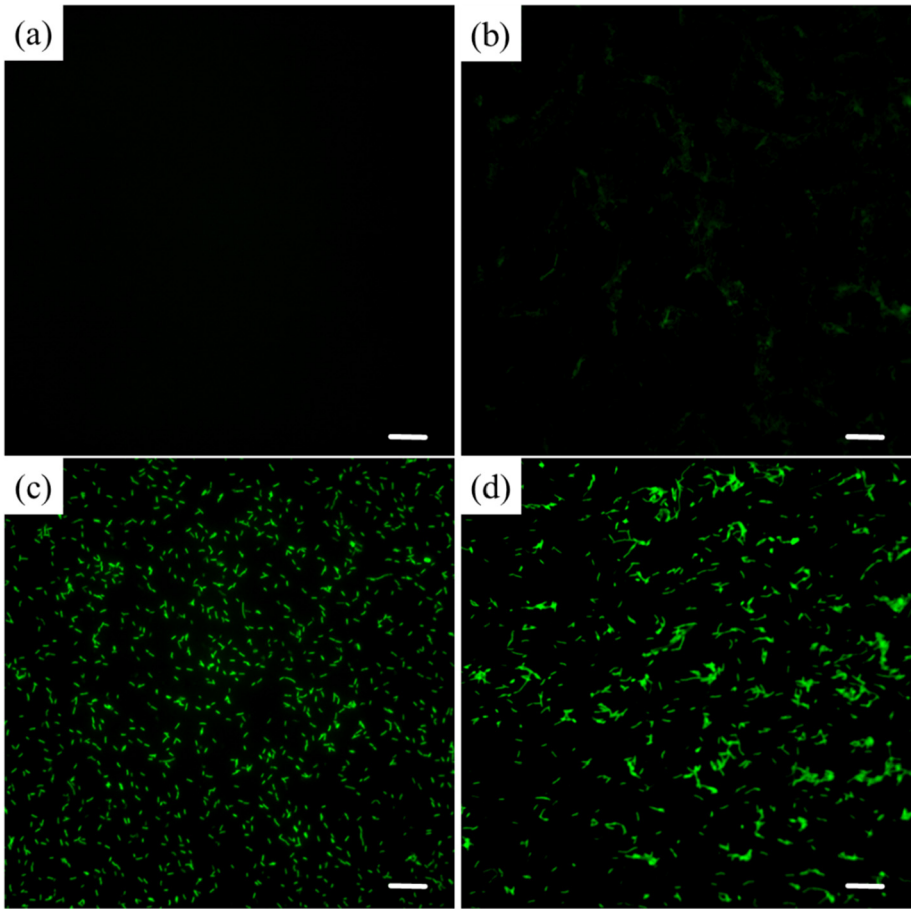

Fig. 7 Fluorescence images of *Xoo* stained with the nonfluorescent oxidation-responsive dye DCFH-DA after treatment with elevated dosages of $\mathbf{D_3}$ (a) 0 μg/mL, (b) 12.5 μg/mL, (c) 25 μg/mL, and (d) 50 μg/mL. Scale bars for (a)–(d) are 10 μm.

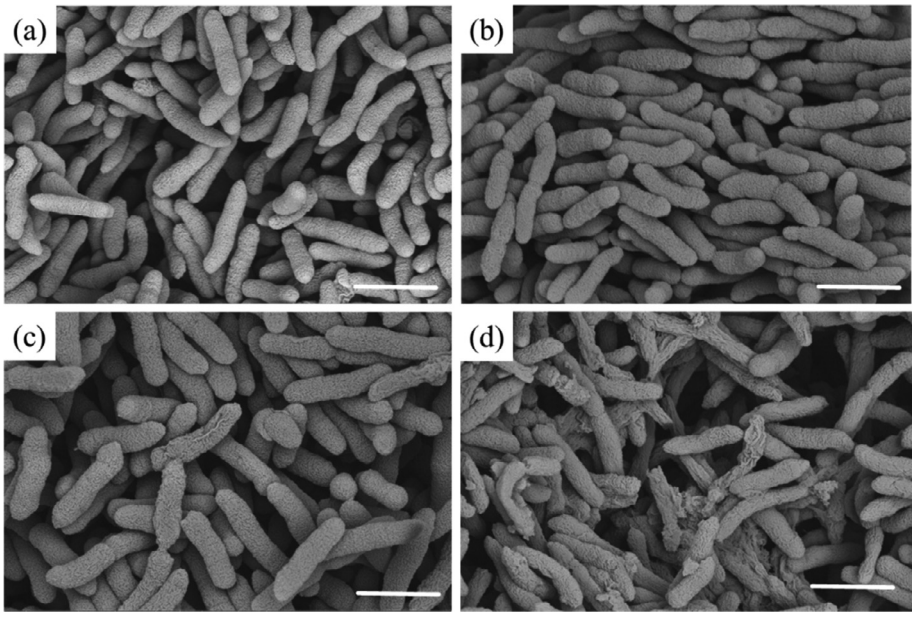

Fig. 8 SEM images for *Xoo* after incubation with various concentrations of $\mathbf{D_3}$. (a) 0 μg/mL, (b) 6.25 μg/mL, (c) 12.5 μg/mL, and (d) 25 μg/mL. Scale bars for (a)–(d) are 10 μm.

pathogens was detected using the fluorescent probe DCFH-DA in this experiment. The results showed (Fig. 7) that ROS levels obviously increased in *Xoo* cells in a concentration-dependent manner when incubated with compound **D_3** for 12 h, which was higher than that of the control group (0 μg/mL). These findings suggested that our designed compounds could interfere with the balance of the redox system in phytopathogenic bacteria, resulting in massive accumulation of ROS, inducing an apoptotic response, and ultimately leading to bacterial death.

3.7. SEM images of bacterial morphological changes

SEM was used to observe the morphological changes of *Xoo* pathogens treated with different concentrations of compound **D_3**. The results (Fig. 8) showed that the morphology of the bacterial cell membrane was indeed affected by compound **D_3**. Compared to the control group (Fig. 8**a**), the surface of *Xoo* cells showed a noticeable shrinkage and depression when treated with compound **D_3**, and the phenomenon became more evident with elevated concentrations (Fig. 8**b-d**). Altogether, these findings showed that compound **D_3** had a considerable ability to affect physiological and biochemical processes, including altering the bacterial defense system, promoting ROS accumulation, and leading to morphological changes, which are consistent with the mechanisms of cell apoptosis.

4. Conclusion

In summary, a class of novel pyridinium salt-decorated 18β-glycyrrhetinic derivatives were designed, synthesized, and their structures were optimized. The results of the antibacterial bioassay showed that compounds **D_3** and **D_8** could efficiently attack two pernicious phytopathogenic bacteria, including *Xoo* and *Xac*, with EC_{50} values of 1.60 and 2.07 μg/mL, respectively. The pot experiment revealed that compound **D_3** had excellent curative and protective activities *in vivo* for the management of rice bacterial blight at 200 μg/mL, of 54.09% and 38.50%, respectively. The phytotoxicity test showed compound **D_3** had markedly lower phytotoxicity than **B_6**, which suggested that the ion exchange method was a feasible means to reduce the adverse effects of pyridinium salt on the plant. Furthermore, AO/EB double staining assays indicated that these compounds could induce strong apoptotic effects on pathogens tested at lower drug concentrations. ROS detection studies showed that compound **D_3** could remarkably induce ROS production in bacteria, which in turn interfered with the bacterial redox system, caused irreversible damage, contraction of the bacterial cell membrane, and finally bacterial death. SEM observations showed that our designed compounds could cause bacteria cell shrinkage and depression, effects which were in accordance with the phenomenon of apoptosis. Overall, the findings suggest that these novel types of pyridinium salt-decorated 18β-glycyrrhetinic derivatives may act as a reference for the development of new bactericide alternatives and provide a rationale for overcoming the limitations in the application of pyridinium salts in agricultural and medical development.

CRediT authorship contribution statement

Jing-Jing He: Writing – original draft, Investigation, Data curation. **Ting Li:** Data curation. **Hong-Wu Liu:** Writing – review & editing. **Lin-Li Yang:** Data curation. **Yi-Hong Yang:** Data curation. **Qing-Qing Tao:** Data curation. **Xiang Zhou:** Resources, Funding acquisition, Writing – review & editing. **Pei-Yi Wang:** Methodology. **Song Yang:** Conceptualization, Funding acquisition, Project administration, Resources, Validation, Writing – review & editing.

Declaration of Competing Interest

The authors declare that they have no known competing financial interests or personal relationships that could have appeared to influence the work reported in this paper.

Acknowledgments

We acknowledge the supports from National Natural Science Foundation of China (21877021, 32160661, 32202359), the Guizhou Provincial S&T Project (2018[4007]), the Guizhou Province [Qianjiaohe KY number (2020)004], Program of Introducing Talents of Discipline to Universities of China (D20023, 111 Program) and GZU (Guizhou University) Found for Newly Enrolled Talent (No. 202229).

Appendix A. Supplementary material

Supporting information including ^{1}H NMR, ^{13}C NMR and HRMS spectra associated. Supplementary data to this article can be found online at https://doi.org/10.1016/j.arabjc.2023.104771.

References

Bodor, N., Kaminski, J.J., Selk, S., 1980. Soft drugs. 1. Labile quaternary ammonium salts as soft antimicrobials. J. Med. Chem. 23 (5), 469–474. https://doi.org/10.1021/jm00179a001.

Butler, M.S., 2005. Natural products to drugs: natural product derived compounds in 300 clinical trials. Nat. Prod. Rep. 22 (2), 162–195. https://doi.org/10.1039/b402985m.

Camp, D., Davis, R.A., Campitelli, M., Ebdon, J., Quinn, R.J., 2012. Drug-like properties: guiding principles for the design of natural product libraries. J. Nat. Prod. 75 (1), 72–81. https://doi.org/10.1021/np200687v.

Chen, G., Cai, Y.G., Xie, X.L., 2021. Occurrence conditions and influencing factors of bacterial diseases in rice. Mod. Agric. Sci. Technol. 120 (21), 116–117. https://doi.org/10.3969/j.issn.1007−5739.2021.21.043.

Chen, M.M., Chen, L.Z., 2022. Plant bacterial diseases and their control measures. J. Zhejiang Agric. Sci. 63 (08). https://doi.org/10.16178/j.issn.0528-9017.20220517.

Chen, Y., Ma, Y., He, Q., Han, Q.X., Zhang, Q., Chen, Q., 2019. Construction of pyridinium/*N*-chloramine polysiloxane on cellulose for synergistic biocidal application. Cellulose. 26 (8), 5033–5049. https://doi.org/10.1007/s10570-019-02437-6.

Dai, L.H., Li, J., Yang, J.G., Men, Y., Zeng, Y., Cai, Y., Sun, Y.X., 2018. Enzymatic synthesis of novel glycyrrhizic acid glucosides using a promiscuous bacillus glycosyltransferase. Catalysts 8 (12), 615. https://doi.org/10.3390/catal8120615.

Fahs, S., Rowther, F.B., Dennison, S.R., Patil-Sen, Y., Warr, T., Snape, T.J., 2014. Development of a novel, multifunctional, membrane-interactive pyridinium salt with potent anticancer activity. Bioorg. Med. Chem. Lett. 24 (15), 3430–3433. https://doi.org/10.1016/j.bmcl.2014.05.087.

Feng, Q., 2021. Discussion on green control of citrus canker. Plant Prot. Sci. 41 (8), 96–98. https://1672-6820(2021)08-0096-03.

Gaware, R., Khunt, R., Czollner, L., Stanetty, C., Da Cunha, T., Kratschmar, D.V., Odermatt, A., Kosma, P., Jordis, U., Classen-Houben, D., 2011. Synthesis of new glycyrrhetinic acid derived ring

A azepanone, 29-urea and 29-hydroxamic acid derivatives as selective 11beta-hydroxysteroid dehydrogenase 2 inhibitors. Bioorg. Med. Chem. 19 (6), 1866–1880. https://doi.org/10.1016/j.bmc.2011.02.005.

Guo, B.Y., 1998. Cell and molecular biology experiment operation guide. Ac. J. Sec. Mil. Med. Univ. 18 (006), 551.

He, H.L., Li, N.J., Sun, C.C., Teng, K., Tian, M.H., Li, S.L., 2021. Research progress in biological control of tobacco bacterial wilt. Plant Doctor. 34 (2), 4–8. https://doi.org/10.13718/j.cnki.zwys.2021.02.002.

Hu, C.X., 2022. Etiology and control measures of bacterial stripe disease in rice. Seed Sci. Technol. 40 (05), 97–99. https://doi.org/10.19904/j.cnki.cn14-1160/s.2022.05.032.

Huang, X., Liu, H.W., Long, Z.Q., Li, Z.X., Zhu, J.J., Wang, P.Y., Qi, P.Y., Liu, L.W., Yang, S., 2021. Optimization of 1,2,3-triazole-tailored carbazoles as prospective antibacterial alternatives with significant *in vivo* control efficiency and unique mode of action. J. Agric. Food. Chem. 69 (16), 615–4627. https://doi.org/10.1021/acs.jafc.1c00707.

Huang, X.W., Sang, S., Lin, W.Q., Cao, Y.H., 2017. Control effect of three copper preparations on pepper bacterial wilt. Modern Agrochem. 16 (1). https://doi.org/10.3969/j.issn.1671-5284.2017.01.014.

Huang, J.Y., Yang, L.D., Su, C.H., Chu, X.W., Zhang, J.Y., Deng, S. P., Cheng, K.G., 2018. Synthesis and cytotoxicity evaluation of pentacyclic triterpene-phenol nitrogen mustard conjugates. Chem. Nat. Compd. 54 (1), 106–111. https://doi.org/10.1007/s10600-018-2270-x.

Hussain, H., Green, I.R., Shamraiz, U., Saleem, M., Badshah, A., Abbas, G., Rehman, N.U., Irshad, M., 2018. Therapeutic potential of glycyrrhetinic acids: a patent review (2010–2017). Expert Opin. Ther. Pat. 28 (5), 383–398. https://doi.org/10.1080/13543776.2018.1455828.

Hüter, O.F., 2011. Use of natural products in the crop protection industry. Phytochem. Rev. 10 (2), 185–194. https://doi.org/10.1007/s11101-010-9168-y.

Jager, S., Trojan, H., Kopp, T., Laszczyk, M.N., Scheffler, A., 2009. Pentacyclic triterpene distribution in various plants-rich sources for a new group of multi-potent plant extracts. Molecules 14 (6), 2016–2031. https://doi.org/10.3390/molecules14062016.

Joo, Y.E., 2014. Natural product-derived drugs for the treatment of inflammatory bowel Diseases. Intest. Res. 12 (2), 103–109. https://doi.org/10.5217/ir.2014.12.2.103.

Kasibhatla, S., Amarante-Mendes, G.P., Finucane, D., Brunner, T., Bossy-Wetzel, E., Green, D.R., 2006. Acridine orange/ethidium bromide (AO/EB) staining to detect apoptosis. Cold Spring Harb. Protoc. 2006 (3), 799–803. https://doi.org/10.1101/pdb.prot4493.

Lei, Y.Y., Kong, Y.D., Sui, H., Feng, J., Zhu, R.Y., Wang, W.P., 2016. Enhanced oral bioavailability of glycyrrhetinic acid via nanocrystal formulation. Drug Deliv. Transl. Res. 6 (5), 519–525. https://doi.org/10.1007/s13346-016-0300-4.

Li, L., Zhong, C.H., Li, D.V., Zhang, S.J., Huang, H.W., 2013. Research progress of kiwifruit bacterial ulcer disease. J. Huazhong Agric. Univ. 32 (5), 124–133. https://doi.org/10.13300/j.cnki.hnlkxb.2013.05.015.

Luo, K., Cai, H.L., Zhou, Z.C., Xiao, L.P., Xiao, Q.M., Li, X., Tang, Q.J., 2015. Research on the prevention and treatment of Tangerine Rhizoma disease. Mod. Agric. Sci. Technol. (8), 123–124. https://1007-5739(2015)08-0123-02.

Marrone, P.G., 2019. Pesticidal natural products-status and future potential. Pest. Manag. Sci. 75, 2325–2340. https://doi.org/10.1002/ps.5433.

Mehraj, U., Mir, I.A., Hussain, M., Alkhanani, M., Na, M.N., Ma, M., 2022. Adapalene and doxorubicin synergistically promote apoptosis of TNBC cells by hyperactivation of the ERK1/2 pathway through ROS induction. Front. Oncol. 12,. https://doi.org/10.21203/rs.3.rs-1590566/v1 938052.

Radwan, M.O., Ismail, M.A., El-Mekkawy, S., Ismail, N.S., Hanna, A.G., 2016. Synthesis and biological activity of new 18β-glycyrrhetinic acid derivatives. Arab. J. Chem. 9 (3), 390–399. https://doi.org/10.1016/j.arabjc.2013.06.032.

Schoenberg, A., Bartoletti, I., Heck, R.F., 1974. Palladium-catalyzed carboalkoxylation of aryl, benzyl, and vinylic halides. J. Org. Chem. 39 (10), 3318–3326. https://doi.org/10.1021/acs.joc.2c00634.

Song, Y.L., Liu, H.W., Yang, Y.H., He, J.J., Yang, B.X., Yang, L.L., Song, Y., 2022. Novel 18β-glycyrrhetinic acid amide derivatives show dual-acting capabilities for control of plant bacterial diseases through ROS-mediated antibacterial efficiency and activation of plant defense responses. J. Integr. Agr. 12 (21). https://doi.org/10.1016/j.jia.2022.10.009.

Sun, J., Liu, H.Y., Lv, C.Z., Qin, J., Wu, Y.F., 2019. Modification, antitumor activity, and targeted PPARγ study of 18β-glycyrrhetinic acid, an important active ingredient of licorice. J. Agric. Food. Chem. 67 (34), 9643–9651. https://doi.org/10.1021/acs.jafc.9b03442.

Sundararaman, M., Kumar, R.R., Venkatesan, P., Ilangovan, A., 2013. 1-Alkyl-(*N*, *N*-dimethylamino) pyridinium bromides: inhibitory effect on virulence factors of Candida albicans and on the growth of bacterial pathogens. J. Med. Microbiol. 62 (2), 241–248. https://doi.org/10.1099/jmm.0.050070-0.

Thorsteinsson, T., Loftsson, T., Masson, M., 2003. Soft antibacterial agents. Curr. Med. Chem. 10 (13), 1129–1136. https://doi.org/10.2174/0929867033457520.

Tian, Q., Wang, X.H., Wang, W., Zhang, C.N., Wang, P., Yuan, Z., 2012. Self-assembly and liver targeting of sulfated chitosan nanoparticles functionalized with glycyrrhetinic acid. Nanomed-Nanotechnol. 8 (6), 870–879. https://doi.org/10.1016/j.nano.2011.11.002.

Wang, P.Y., Xiang, M., Luo, M., Liu, H.W., Zhou, X., Wu, Z.B., Liu, L.W., Li, Z., Yang, S., 2020. Novel piperazine-tailored ursolic acid hybrids as significant antibacterial agents targeting phytopathogens *Xanthomonas oryzae* pv. *oryzae* and *X. axonopodis* pv. *citri* probably directed by activation of apoptosis. Pest. Manag. Sci. 76 (8), 2746–2754. https://doi.org/10.1002/ps.5822.

Wang, F., Yang, B.X., Zhang, T.H., Tao, Q.Q., Zhou, X., Wang, P.Y., Yang, S., 2022. Novel 1, 3, 4-Oxadiazole thioether and sulfone derivatives bearing a flexible N-heterocyclic moiety: synthesis, characterization, and anti-microorganism activity. Arab. J. Chem. 2 (16), 104479. https://doi.org/10.1016/j.arabjc.2022.104479.

Wu, S.C., Liu, F., Zhu, K., Shen, J.Z., 2019. Natural products that target virulence factors in antibiotic resistant *Staphylococcus aureus*. J. Agric. Food Chem. 67 (48), 13195–13211. https://doi.org/10.1021/acs.jafc.9b05595.

Xiang, M., Song, Y.L., Ji, J., Zhou, X., Liu, L.W., Wang, P.Y., Wu, Z. B., Li, Z., Yang, S., 2020. Synthesis of novel 18β-glycyrrhetinic piperazine amides displaying significant *in vitro* and *in vivo* antibacterial activities against intractable plant bacterial diseases. Pest Manage. Sci. 76 (9), 2959–2971. https://doi.org/10.1002/ps.5841.

Xu, X., Hou, X.D., Jiang, S.C., 2021. Research progress on green control technology of soil-borne diseases of pepper in protected areas. Anhui Agric. Sci. Bull. 27 (23), 121–123. https://doi.org/10.16377/j.cnki.issn1007-7731.2021.23.033.

Xu, Q.M., Liu, Y.L., Feng, Y.L., Tang, L.H., Yang, S.L., 2012. A new E-ring gamma-lactone pentacyclic triterpene from *Lysimachia clethroides* and its cytotoxic activities. Chem. Nat. Compd. 48 (4), 597–600. https://doi.org/10.1007/s10600-012-0321-2.

Yang, Y., Zhu, Q.Y., Zhong, Y.Y., Cui, X.P., Jiang, Z.Y., Wu, P.P., Zheng, X., Zhang, K., Zhao, S.Q., 2020. Synthesis, anti-microbial and anti-inflammatory activities of 18β-glycyrrhetinic acid derivatives. Bioorg. Chem. 101. https://doi.org/10.1016/j.bioorg.2020.103985.

Zhang, Y., Dai, S.M., Long, G.Y., Zhou, M., Sun, T.A., Li, D.Z., 2021. Occurrence and control status of main diseases and insects in

citrus in Hunan Province. Hunan Agric. Sci. 12, 61–64. https://doi.org/10.16498/j.cnki.hnnykx.2021.012.016.

Zhang, L.Y., Dong, J.Z., Liu, J., Zhang, L.Y., Kong, L.Y., Yao, H.Q., Sun, H.B., 2013. Synthesis and biological evaluation of novel pentacyclic triterpene derivatives as potential PPAR gamma agonists. Med. Chem. 9 (1), 118–125. https://doi.org/10.2174/1573406411309010118.

Zhao, J., Cai, W.L., Shen, L.Y., Zhu, H.Y., Pu, L., Xie, M.Q., Zhou, Y.L., Hua, H.X., 2022. Research status and prospect of green pest control technology in rice. J. Huazhong Agric. Univ. 41 (1), 92–104. https://doi.org/10.13300/j.cnki.hnlkxb.2022.01.009.

Zhao, Y.L., Huang, X., Liu, L.W., Wang, P.Y., Long, Q.S., Tao, Q. Q., Li, Z., Yang, S., 2019. Identification of racemic and chiral carbazole derivatives containing an isopropanolamine linker as prospective surrogates against plant pathogenic bacteria: *in vitro* and *in vivo* assays and quantitative proteomics. J. Agric. Food. Chem. 67 (26), 7512–7525. https://doi.org/10.1021/acs.jafc.9b02036.

Zhao, T., Sun, G., 2006. Synthesis and characterization of antimicrobial cationic surfactants: aminopyridinium salts. J. Surfactants Deterg. 9 (4), 325–330. https://doi.org/10.1007/s11743-006-5010-3.

Zhen, H., Xu, S.J., Yang, X.X., Chen, Z.L., 2011. Progress of research on antimicrobial agents and their application to textiles. Text. Res. J. 32 (11), 153–161. https://doi.org/10.13475/j.fzxb.2011.11.018.

Zígolo, M.A., Salinas, M., Alché, L., Baldessari, A., Liñares, G.G., 2018. Chemoenzymatic synthesis of new derivatives of glycyrrhetinic acid with antiviral activity molecular docking study. Bioorg. Chem. 78, 210–219. https://doi.org/10.1016/j.bioorg.2018.03.018.